RSC Advances

ROYAL SOCIETY OF CHEMISTRY

www.rsc.org/advances

First-principle study on the phase transition temperature of X-doped (X = Li, Na or K) VO_2

Yuanyuan Cui,[1] Yongxin Wang,[1] Bin Liu,[1] Hongjie Luo,[1] and Yanfeng Gao[1,2,a)]

[1] *School of Materials Science and Engineering, Shanghai University, Shanghai 200444, China*

[2] *Huaiyin Institute of Technology, No.1 Eastern Meicheng Rd., Huaian, Jiangsu, 223003, China*

Abstract

Vanadium dioxide (VO_2) is one of the most interesting thermochromic materials with a phase transition temperature of 340 K. Our first-principles calculation indicates that Li, Na or K dopants with a doping level of 1 atomic percentage could reduce the phase transition temperature of VO_2 by 43K, 49K, 94 K, respectively. In addition, the V-V chains feature the dimerization characteristics in the Li, Na or K doped VO_2(R). The calculated electronic structures and optical properties indicate that K is as an appropriate doping element for VO_2, since it can effectively lower the phase transition temperature as well as enhance the near-infrared absorption.

Keywords: Vanadium dioxide; Alkali doping; Phase transition temperature; First-principles calculation

[a)] Corresponding authour's E-mail address: yfgao@shu.edu.cn (Yanfeng Gao)

1. Introduction

Smart windows refer to a glass window that can intelligently control the amount of light and heat passing through, usually by an external stimulus such as electrical field (electrochromic), temperature (thermochromic), ultraviolet irradiation (photochromic) and reductive or oxidizing gases (gasochromic).[1] Vanadium oxide is an abundant and diverse family of compounds with thermochromic properties, among which V_2O_3, VO_2 and V_2O_5 could undergo a metal-insulator phase transitions (MIT) at the critical temperatures of 168 K, 340 K and 145 K, respectively.[2,3] Table 1 summarizes the basic physical properties of V_2O_3, VO_2 and V_2O_5.[2]

Vanadium dioxide (VO_2), as a key material of thermochromic smart windows, has been consistently studied since the discovery of its MIT at ~340 K in 1959.[4,5] Across the MIT from the low-temperature monoclinic (M) phase to the high-temperature rutile (R) phase, VO_2 undergoes a transition from a relative infrared transparent state to an infrared reflecting state, which is accompanied by an abrupt resistivity change.[6,7] This property can be exploited to intelligently control near-infrared light radiation, which carries a large amount of solar energy, and makes VO_2 a promising material for use in smart windows.[8-10]

The phase transition temperature (T_c) is approximately 340 K for pure VO_2, and it should be lowered to near room temperature (298 K) in order to meet the requirement of the applications of VO_2 for smart windows.[11] To address this issue, various studies have been conducted to tailor T_c by means of element doping,[12] external strain,[13] photon irradiation[14] or a combination of these factors.[15] Reported results reveal a significant

evidence that the properties of VO_2 could be effectively influenced through doping special elements such as H, W, Mo or Nb.[16-19] For instance, H-doped VO_2 film was reported to present the metallic properties when cooled down to 120 K, and the change of T_c is around -55 K/at.% H (at.% means per atomic percentage).[16] W is proven to be one of the most effective dopants where the transition temperature is reduced by about 28 K with increase of every 1 at.% of W.[17] The Mo-doped VO_2 nanowires synthesized through melting-quenching method presented the decreased T_c to 315 K.[18] The dopant-induced reduction of T_c in VO_2 can be concisely explained as follows: the doped atoms provide or remove some of their electrons in the V 3d valence bands and make some V-V pairs break in M-phase, which leads to the destabilization of VO_2 and consequently lowers the MIT temperature.

It was revealed that the reduction of T_c mentioned above is essentially attributed to injected carriers from dopants.[20] More additional electrons provided from the doped atoms favor a decrease in MIT temperature. For instance, first-principles calculations indicate that Be doping can change the electronic structure by injecting additional electrons which reduce the transition temperature by 58 K per at% Be.[20] Motivated by this finding, we herein propose a new strategy to modulate the transition temperature of VO_2 by doping with the most frequently used alkali, *i.e.*, Li, Na or K, which possesses one electron in the outermost orbital. Doping at an interstitial site can inject this electron into a VO_2 supercell, which may reduce MIT temperature.

2. Computational details

Calculations were conducted with the Vienna *ab* initio simulation package (VASP),

a plane wave density functional code.[21,22] The potentials were of the projector augmented wave (PAW) type, and the exchange-correlation part of the density functional was treated within the generalized gradient approximation (GGA) of Perdew-Burke-Ernzerhof (PBE).[23,24] To account for strong on-site Coulomb repulsion among the V 3*d* electrons for VO_2(M), [25,26] the Hubbard parameter *U* was added to the PBE functional in the rotationally invariant approach of Dudarev *et al*., in which only the difference (U_{eff}=*U*-*J*) between the Coulomb repulsion *U* and screened exchange *J* parameters must be specified.[27,28] Despite the fact that more sophisticated methods such as GW, local density approximation with dynamical mean field theory (LDA+DMFT) and particular hybrid functionals might yield better results,[29-32] the Dudarev DFT+*U* method has been shown to reasonably describe the electronic structure and strong correlation of VO_2(M). For instance, Zhang *et al*. correctly predicted that both VO_2(R) and VO_2(M) phases were energetically stabilized by Be doping using the GGA+*U* method,[20] and Sun *et al*. successfully reproduced that W, Mo, and Re were the most effective dopants to reduce the T_c of VO_2.[33] As discussed in references,[17,20] U_{eff} in GGA+*U* formalism was chosen to be 3.4 eV in the present calculations.

The valence electron configurations for the elemental constituents are as follows: V-$3d^3 4s^2$, O-$2s^2 2p^4$, Li-$2s^1$, Na-$3s^1$, K-$4s^1$. The cut-off energy for the plane-wave basis was 520 eV. The basic calculations were performed in the supercells with 2×2×4 and 2×2×2 primitive unit cells for the VO_2(R) and VO_2(M) phase, respectively. Each supercell consisted of 96 atoms, with one Li, Na or K atom doped at one of three different interstitial sites: the tetrahedral (T), octahedral (O) and side centered (S) site as

shown in Fig. 1. In comparison, the doped atom substituted the V site was also taken into considerations. 2×3×3 *k*-point meshes were used to sample the Brillouin zone for the different sized supercells. This set of parameters assured that the total energies converged to 1×10^{-5} eV/unit cell. Lattice constants and internal coordinates are fully optimized until Hellmann-Feynman forces became less than 0.01 eV/Å.

3. Results and Discussion

3.1 Reduction in phase transition temperature

To compare the relative stability among the alkali dopants in the different interstitial sites of VO_2, interstitial formation energy, E_i, is calculated *via*

$$E_i = E_{doped} - E_{pure} - xE_{alkali}, \quad (1)$$

where E_{pure} and E_{doped} correspond to the total energy of the pure and doped VO_2 supercell, respectively. E_{alkali} is the total energy per atom of the optimized Li, Na or K metal, and x is the number of doped atoms in one supercell.

Table 2 contains the available calculated and experimental results of the lattice constants, interstitial formation energies (E_i) of Li, Na or K at different interstitial sites, supercell volumes, enthalpies and band gaps of VO_2. It can be seen from the table that the enthalpies of VO_2(M) and VO_2(R) are -699.613 eV/supercell and -704.748 eV/supercell, respectively, which implies that the VO_2(R) is more stable than VO_2(M), agreeing well with the experiments.[34] Moreover, Li, Na or K doping into VO_2(R) or VO_2(M) interstitial sites is an exothermal process due to the reason that all E_i values are negative. Then, we compare the E_i of different doping interstitial sites. In fact, we set a tight convergence criterion in the calculations which assured that the relaxation of the

electronic loop stopped when the total energies change between two steps were smaller than 1×10^{-5} eV/unit supercell, and the lattice constants and internal coordinates were fully optimized until Hellmann-Feynman forces became less than 0.01eV/Å, so that the energies are calculated with high accuracy. Therefore, the energy differences of dopants at different sites should not be treated as errors although the values are small.

It can be seem from Table 2 that VO_2(M) with Li, Na and K at the T site, the O site and the O site has the lowest E_i, respectively, suggesting the most possible doping site of Li, Na and K in VO_2 is the T site, the O site and the O site, respectively. The interstitial size of the T site and O site in VO_2 are 0.70 Å and 1.21 Å, respectively. The doping Li, Na or K atom has a radius of 0.68 Å, 0.97 Å and 1.33 Å, respectively.[35] The atomic radius of Li is close to that of the T site and the distortion caused by Li atom at the T site is found to be less than that at the O site, accordingly, the Li atom is easier to occupy the T site in VO_2. For Na or K doped systems, the atomic radius of the dopant is larger than that of the T site but smaller than that of the O site，therefore the Na or K atom is easier to occupy the O site in VO_2. For the sake of simplicity, the results of VO_2 with Li, Na and K at the octahedral (T) site, the two octahedral (O) sites were taken as representatives in the following discussion, respectively.

The influence of the Li, Na or K on the phase transition temperature (T_c) can be quantitatively calculated according to the thermodynamic model of Netsianda *et al*,[38] in which the T_c upon doping is given via

$$T_c = T_{c,0}\frac{\Delta H}{\Delta H_0} \quad (2)$$

where $T_{c,0}$ is the transition temperature of pure VO_2, and the value of 340 K was

adopted. ΔH and ΔH_0 are the enthalpy changes associated with the phase transition for doped and pure VO_2, respectively.[38] The enthalpy was approximated as the Helmholtz free energy obtained from our DFT calculations by neglecting the pV term for condensed matter and omitting the contribution from entropy at 0 K. This thermodynamic model of Netsianda *et al* has been successfully applied to a number of research results.[17,20] For instance, Zhang *et al*. estimated the reduction of T_c to be 27 K/at.% by W doping, which is quite close to 20~26 K/at.% observed in experiments.[17] The transition temperature change between the doped and pure VO_2 can be defined as

$$\Delta T_c = T_c - T_{c,0} \quad (3)$$

From Equations (2) and (3), it can be calculated that Li, Na or K dopants with a doping level of 1 atomic percentage could reduce T_c by 43K, 49K, 94 K, respectively

3.2 Atomic and electronic structures on pure and doped VO_2

The V-V chains along *c*-axis described in Fig. 2(a) shows that the V atoms arrange uniformly with a distance of 2.789 Å in pure VO_2(R). Fig. 2(b) shows that the V-V bonds arrange alternately at 3.125 Å and 2.654 Å along *c*-axis due to the existence of Peierls distortion in pure VO_2(M). As the three doping structures present the same change trend, we take the K-doped structure as an example. Fig. 2(g) shows the structural distortion of K-doped VO_2(R) phase, the distance of V-V bonds range from 2.935 Å to 3.026 Å, and the short ones range from 2.486 Å to 2.692 Å. Fig. 2(h) describes the short V-V distance in the K-doped VO_2(M) range from 2.468 Å to 2.523 Å, and the long distance range from 2.860 Å to 3.119 Å. It can be seen from Fig. 2 that all of the Li, Na or K-doped VO_2(R) phases all feature the dimerization characteristics as

that in VO_2(M) phase. Moreover, the Li, Na or K doping has a greater influence on the atomic structures of VO_2(R) with respect to that of VO_2(M).

In this section, we will discuss the electronic structures on the pure and doped VO_2. Fig. 3 describes the density of states (DOS) of pure VO_2 and Li, Na or K doped VO_2. It can be seen from Fig. 3(a), (c), (e) and (g) that the pure, Li, Na and K doped VO_2(R) exhibit the metallic properties since the Fermi level crosses the conduction band. Fig. 3(b) is the density of states of the pure VO_2(M), showing that the Fermi level of exists in the top of valence band with a band gap of 0.61 eV, close to the X-ray photoemission data[39] and other theoretical calculation results.[39,40]. Fig. 3(d) and (f) show a shifting up of Fermi level to the edge of the conduction band and a widened band gap of 0.734 eV and 0.714 eV. Fig. 3(h) shows that K-doped VO_2(M) has a narrowed band gap of 0.562 eV. Generally, the intrinsic band gap has an impact on the near-infrared (800~1500 nm) absorption of the VO_2 film, the widened band gap for Li or Na doped VO_2(M) is expected to result in an decrease in the near-infrared absorption, while the narrowed band gap for K doped VO_2(M) may lead to an increase in the near-infrared absorption. Based on the discussion above, the K can be selected as an appropriate doping element for VO_2, since it can lower the phase transition temperature as well as enhance the near-IR absorption

Fig. 4 shows the V 3d partial DOS in both pure VO_2 and K-doped VO_2. In the atomic structure of VO_2, each V atom of VO_2 is surrounded by a distorted VO_6 octahedron. This structure leads to a splitting of the d level to doubly degenerate e_g^{σ} and triply degenerate t_{2g} states. The two components states are labeled as $d_{x^2-y^2}$ and

d_{z^2}, whereas the three components of the triply degenerate t_{2g} states are signed as d_{xy}, d_{yz}, and d_{xz}.[40] Fig. 4(a) and (b) show the pure and K-doped VO_2 with blue and red line, respectively. The occupied states of the doped system all extend to the lower energies, showing that the V 3d orbitals have stronger bonding. As mentioned above, the V atoms in VO_2(R) are equally spaced along the *c*-axis, and those in VO_2(M) are dimerized and tilted with respect to the *c*-axis (Fig. 2). We should focus on the d_{z^2} orbital because the V-V chain extends along the *c*-direction which is the V–V chain direction in VO_2. Fig. 4(a) shows that the occupied states of d_{z^2} shift down to -1.26 eV and the unoccupied states raise up to 1.54 eV in K-doped VO_2(R) with respect to that of the pure system, confirming a stronger bonding between the nearest-neighboring V atoms.

3.3 Absorption coefficients of the pure and the K-doped VO_2(M)

The optical properties of a material can be described by means of the dielectric function: $\varepsilon(\omega) = \varepsilon_1(\omega) + i\varepsilon_2(\omega)$.[35] The imaginary part ($\varepsilon_2(\omega)$) of the dielectric function can be regarded as detailing of the real transitions between the occupied and unoccupied electronic states. The real part ($\varepsilon_1(\omega)$) of the dielectric function can be obtained from the imaginary part with the famous Kramers-Kronig relationship. The absorption coefficient ($\alpha(\omega)$) can be derived from $\varepsilon_1(\omega)$ and $\varepsilon_2(\omega)$, which are calculated *via*:[35]

$$\alpha(\omega) = \frac{\omega}{c}\left[2\sqrt{\varepsilon_1^2(\omega)+\varepsilon_2^2(\omega)} - 2\varepsilon_1(\omega)\right]^{\frac{1}{2}} \quad (4)$$

Since our concerned VO_2(R) and VO_2(M) are both optically anisotropic, the components of the dielectric function, corresponding to the electric field parallel to (notated as $E_{//}$) and perpendicular to (notated as $E_{\perp}$) the V-V chains, have been considered in our calculations. Fig. 5 displays the absorption coefficients of the pure

and the K-doped VO_2(M) for the near infrared light. Fig. 5(a) shows a weak absorption for the pure VO_2(M), indicating that infrared light could easily penetrate the VO_2(M), in good agreement with the experimental observations. When the systems are doped with K, the VO_2(M) exhibits a larger absorption coefficient for the light with energy less than 1.6 eV in Fig. 3(b), suggesting the introduction of K increases the absorption of the infrared light in VO_2(M). The optical properties of the K-doped VO_2(M) can be explained through its electronic structures. As displayed in Figure 3(h), there is a 0.562 eV band-gap near the bottom of conduction band of K-doped VO_2(M). The infrared light would lead to electronic transitions from the occupied state to the unoccupied states, which just corresponds to the strong absorption for the light with energy less than 1.6 eV.

4. Concluding remarks

In summary, by using first-principles calculation, we investigated the behavior of Li, Na or K-doping and its influence on the transition temperature (T_c) of VO_2. The Li atom is easily located at the tetrahedral interstitial site in VO_2, whereas the Na or K atom is easily located at the octahedral interstitial site, which can be ascribe to different atomic sizes of the dopants. The phase transition temperature of VO_2 can be reduced by 43 K, 49 K or 94 K with 1% of Li, Na or K doping, respectively. The atomic structures show that the V-V chains feature the dimerization characteristics in the Li, Na or K doped VO_2(R). The K can be selected as an appropriate doping alkali for VO_2, since it can lower the phase transition temperature and enhance the near-infrared absorption.

Acknowledgments

The authors gratefully acknowledge the National Natural Science Foundation of China (51372228, 51325203 and 51402182), the Ministry of Science and Technology of China (2014AA032802), the Shanghai Municipal Science and Technology Commission (15XD1501700 and 14DZ2261200) and the high performance computing platform of Shanghai University.

References

1 Y. Gao, C. Cao, L. Dai, H. Luo, M. Kanehira, Y. Ding, and Z. L. Wang, *Energ. Environ. Sci.*, 2012, **5**, 8708.

2 S. Shin, S. Suga, M. Taniguchi, M. Fujisawa, H. Kanzaki, A. Fujimori, H. Daimon, Y. Ueda, K. Kosuge, and S. Kachi, *Phys. Rev. B*, 1990, **41**, 4993.

3 T. Reeswinkel, D. Music, and J. M. Schneider, *J. Phys.-Condes. Matter*, 2009, **21**, 145404.

4 F. J. Morin, *Phys. Rev. Lett.*, 1959, **3,** 34.

5 M. Li, D. B. Li, J. Pan, H. Wu, L. Zhong, Q. Wang, and G. H. Li, *J. Phys. Chem. C,* 2014, **118**, 16279.

6 D. Porwal, A. C. M. Esther, I. N. Reddy, N. Sridhara, N. P. Yadav, D. Rangappa, P. Bera, C. Anandan, A. K. Sharma, and A. Dey, *RSC Adv.*, 2015, **5**, 35737.

7 M. Yang, Y. Yang, B. Hong, L. Wang, Z. Luo, X. Li, C. Kang, M. Li, H. Zong, and C. Gao, *RSC Adv.,* 2015, **5**, 80122.

8 A. I. Maaroof, D. Cho, B. Kim, H. Kim, and S. Hong, *J. Phys. Chem. C*, 2013, **117**, 19601.

9 C. Wu, F. Feng, J. Feng, J. Dai, J. Yang, and Y. Xie, *J. Phys. Chem. C,* 2011, **115**, 791.

10 Q. Cheng, S. Paradis, T. Bui and M. Almasri, *IEEE Sens. J.*, 2011, **11**, 167.

11 Y. Gao, H. Luo, Z. Zhang, L. Kang, Z. Chen, J. Du, M. Kanehira, and C. Cao, *Nano Energy*, 2012, **1**, 221.

12 W. Zhang, K. Wang, L. Fan, L. Liu, P. Guo, C. Zou, J. Wang, H. Qian, K. Ibrahim, W. Yan, F. Xu, and Z. Wu, *J. Phys. Chem. C*, 2014, **118**, 12837.

13 J. Cao, E. Ertekin, V. Srinivasan, W. Fan, S. Huang, H. Zheng, J. W. L. Yim, D. R. Khanal, D. F. Ogletree, J. C. Grossmanan, and J. Wu, *Nat. Nanotechnol.,* 2009, **4**, 732.

14 S. Lysenko, A. Rua, V. Vikhnin, F. Fernandez, and H. Liu, *Phys. Rev. B*, 2007, **76**, 035104.

15 S. Chang, J. B. Park, G. Lee, H. J. Kim, J. Lee, T. Bae, Y. Han, T. J. Park, Y. S. Huh, and W. Hong, *Nanoscale*, 2014, **6**, 8068.

16 V. N. Andreev, V. M. Kapralova and V. A. Klimov, *Phys. Solid State*, 2007, **49**, 2318.

17 J. Zhang, H. He, Y. Xie, and B. Pan, *J. Chem. Phys.,* 2013, **138**, 114705.

18 L. Q. Mai, B. Hu, T. Hu, W. Chen, and E. D. Gu, *J. Phys. Chem. B*, 2006, **110**, 19083.

19 C. Batista, J. Carneiro, R. M. Ribeiro, and V. Teixeira, *J. Nanosci. Nanotechno.*, 2011, **11**, 9042.

20 J. Zhang, H. He, Y. Xie, and B. Pan, *Phys. Chem. Chem.* Phys., 2013, **15**, 4687.

21 G. Kresse and J. Hafner, *Phys. Rev. B*, 1993, **47**, 558.

22 G. Kresse and J. Furthmuller, *Phys. Rev. B*, 1996, **54**, 11169.

23 P. E. Blochl, *Phys. Rev. B*, 1994, **50**, 17953.

24 J. P. Perdew, K. Burke and M. Ernzerhof, *Phys. Rev. Lett.*, 1996, **77**, 3865.

25 R. M. Wentzcovitch, W. W. Schulz and P. B. Allen, *Phys. Rev. Lett.*, 1994, **72**,

3389.

26 T. M. Rice, H. Launois, J. P. Pouget, R. M. Wentzcovitch, W. W. Schulz and P. B. Allen, *Phys. Rev. Lett.*, 1994, **73**, 3042.

27 T. J. Huffman, P. Xu, M. M. Qazilbash, E. J. Walter, H. Krakauer, J. Wei, D. H. Cobden, H. A. Bechtel, M. C. Martin, G. L. Carr and D. N. Basov, *Phys. Rev. B,* 2013, **87**, 115121.

28 S. Kim, K. Kim, C. Kang and B. I. Min, *Phys. Rev. B*, 2013, **87**, 195106.

29 M. S. Laad, L. Craco and E. Mueller-Hartmann, *Phys. Rev. B*, 2006, **73**, 195120.

30 R. Sakuma, T. Miyake and F. Aryasetiawan, *Phys. Rev. B*, 2008, **78**, 75106.

31 V. Eyert, *Phys. Rev. Lett.*, 2011, **107**, 16401.

32 X. Yuan, Y. Zhang, T. A. Abtew, P. Zhang and W. Zhang, *Phys. Rev. B*, 2012, **86**, 235103.

33 C. Sun, L. Yan, B. Yue, H. Liu and Y. Gao, *J. Mater. Chem. C*, 2014, **2**, 9283.

34 G. Guzman, F. Beteille, R. Morineau, and J. Livage, *J. Mater. Chem.*, 1996, **6**, 505.

35 C. Kittel, *Introduction to Solid State Physics*, Wiley, New York, 2002..

36 K. D. Rogers, *Powder Diffr.*, 1993, **8,** 240.

37 J. Zhou, Y. Gao, X. Liu, Z. Chen, L. Dai, C. Cao, H. Luo, M. Kanahira, C. Sun, and L. Yan, *Phys. Chem. Chem. Phys.*, 2013, **15,** 7505.

38 M. Netsianda, P. E. Ngoepe, C. Richard, A. Catlow, and S. M. Woodley, *Chem. Mater.*, 2008, **20**, 1764.

39 T. C. Koethe, Z. Hu, M. W. Haverkort, C. Schuessler-Langeheine, F. Venturini, N. B. Brookes, O. Tjernberg, W. Reichelt, H. H. Hsieh, H. J. Lin, C. T. Chen, and L. H. Tjeng, *Phys. Rev. Lett.*, 2006, **97,** 116402.

40 A. S. Belozerov, M. A. Korotin, V. I. Anisimov, and A. I. Poteryaev, *Phys. Rev. B*, 2012, **85,** 045109.

Table. 1 Comparisons of the properties of V_2O_3, VO_2 and V_2O_5.[2]

	valance	3d electron	crystal structure	T_c (K)	transport (T<Tc)	band gap
V_2O_3	V^{3+}	$3d^2$	Hexagonal	168	*n*-type	~0.2eV
VO_2	V^{4+}	$3d^1$	Monoclinic	340	*n*-type	~0.6eV
V_2O_5	V^{5+}	$3d^0$	Orthorhombic	145	*n*-type	~2eV

Table. 2 The lattice parameters (a, b, c, α, β, γ), interstitial formation energies (E_i) of Li, Na and K in VO_2 at the tetrahedral (T), octahedral (O) and side centered (S) sites, volumes (V), calculated enthalpies (H), and band gaps (E_g) collected from the experiments and the *ab initio* calculations.

	a (Å)	b (Å)	c (Å)	α (°)	β (°)	γ (°)	V (Å^3/atom)	E_i (eV/atom)	H (eV/supercell)	E_g (eV)	
R-phase											
$V_{32}O_{64}$	9.108	9.108	11.428	90	90	90	9.872	-	-	0.000	Expt.[36]
$V_{32}O_{64}$	9.305	9.305	11.154	90	90	90	10.060	-	-	0.000	Calc.[37]
$V_{32}O_{64}$	9.313	9.313	11.156	90	90	90	10.079	-	-699.613	0.000	this work
$LiV_{32}O_{64}$ (T)	9.265	9.323	11.165	90	90	90	10.046	-2.351	-709.837	0.000	this work
$LiV_{32}O_{64}$ (O)	9.276	9.359	11.127	90	90	90	10.062	-2.345	-709.274	0.000	this work
$LiV_{32}O_{64}$ (S)	9.386	9.307	11.148	90	90	90	10.145	-2.345	-709.279	0.000	this work
$NaV_{32}O_{64}$ (T)	9.272	9.342	11.134	90	90	90	10.046	-2.329	-707.119	0.000	this work
$NaV_{32}O_{64}$ (O)	9.291	9.376	11.089	90	90	90	10.062	-2.325	-706.748	0.000	this work
$NaV_{32}O_{64}$ (S)	9.396	9.327	11.113	90	90	90	10.145	-2.326	-706.850	0.000	this work
$KV_{32}O_{64}$ (T)	9.274	9.265	11.224	90	90	90	10.046	-2.683	-741.220	0.000	this work
$KV_{32}O_{64}$ (O)	9.375	9.257	11.133	90	90	88.8	10.062	-2.686	-741.477	0.000	this work
$KV_{32}O_{64}$ (S)	9.289	9.402	11.154	90	90	91.3	10.145	-2.682	-741.082	0.000	this work
M-phase											

$V_{32}O_{64}$	9.052	10.766	11.506	122.6	90	90	9.839	-	-	0.590	Expt.[36]
$V_{32}O_{64}$	9.100	10.600	11.480	122.2	90	90	9.760	-	-	-	Calc.[37]
$V_{32}O_{64}$	9.232	10.867	11.212	121.7	90	90	9.972	-	-704.748	0.610	this work
$LiV_{32}O_{64}$ (T)	9.249	10.924	11.225	121.6	90	90	10.067	-2.384	-713.030	0.734	this work
$LiV_{32}O_{64}$ (O)	9.255	10.930	11.230	121.6	90	90	10.084	-2.384	-713.026	0.738	this work
$LiV_{32}O_{64}$ (S)	9.249	10.924	11.225	121.6	90	90	10.067	-2.382	-713.030	0.715	this work
$NaV_{32}O_{64}$ (T)	9.232	10.932	11.247	121.6	90	90	10.067	-2.308	-705.141	0.487	this work
$NaV_{32}O_{64}$ (O)	9.262	10.937	11.207	121.5	90	90	10.084	-2.359	-710.036	0.714	this work
$NaV_{32}O_{64}$ (S)	9.304	10.883	11.213	121.4	90	90	10.092	-2.357	-709.911	0.682	this work
$KV_{32}O_{64}$ (T)	9.185	10.955	11.268	121.5	90	90	10.067	-2.621	-739.690	0.456	this work
$KV_{32}O_{64}$ (O)	9.335	10.876	11.188	121.5	90	90	10.084	-2.695	-742.356	0.562	this work
$KV_{32}O_{64}$ (S)	9.262	10.924	11.187	121.1	90	90	10.092	-2.683	-741.198	0.489	this work

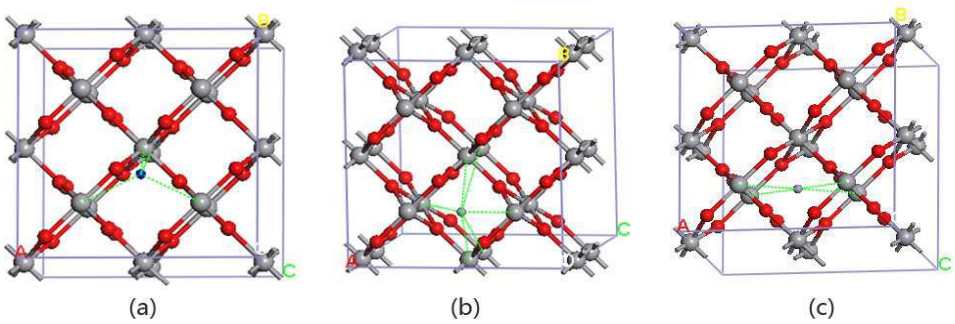

Fig. 1 Tetrahedral (a), octahedral (b) and side-centered (c) interstitial sites in VO_2.The V, O and doped atoms are indicated by gray, red and purple spheres, respectively.

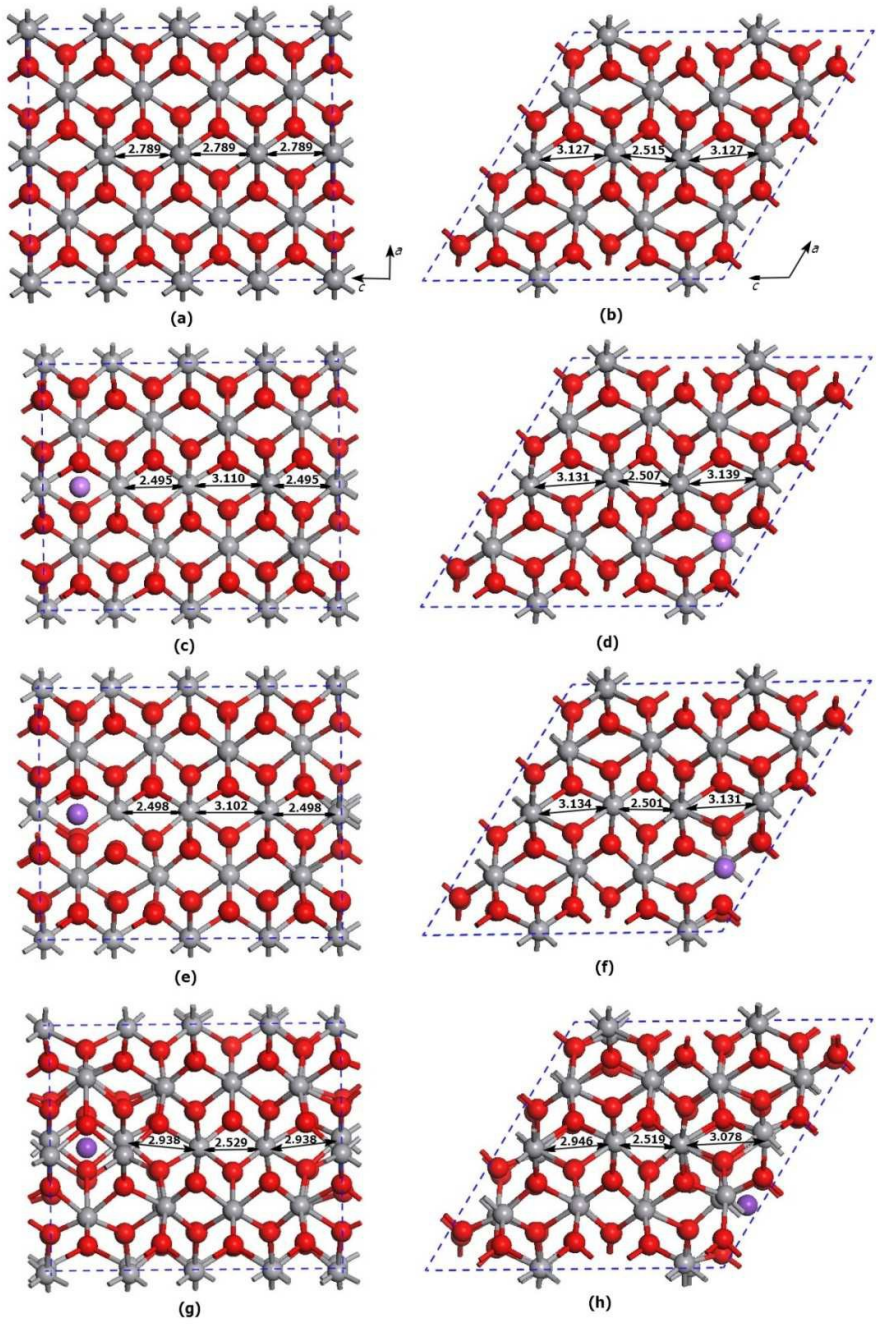

Fig. 2 The V-V chains along *c*-axis for pure VO_2(R) (a), pure VO_2(M) (b), Li-doped VO_2(R) (c) , Li-doped VO_2(M) (d), Na-doped VO_2(R) (e), Na-doped VO_2(M) (f), K-doped VO_2(R) (g) and K-doped VO_2(M) (h). The V, O and doped atoms are indicated by gray, red and purple spheres, respectively.

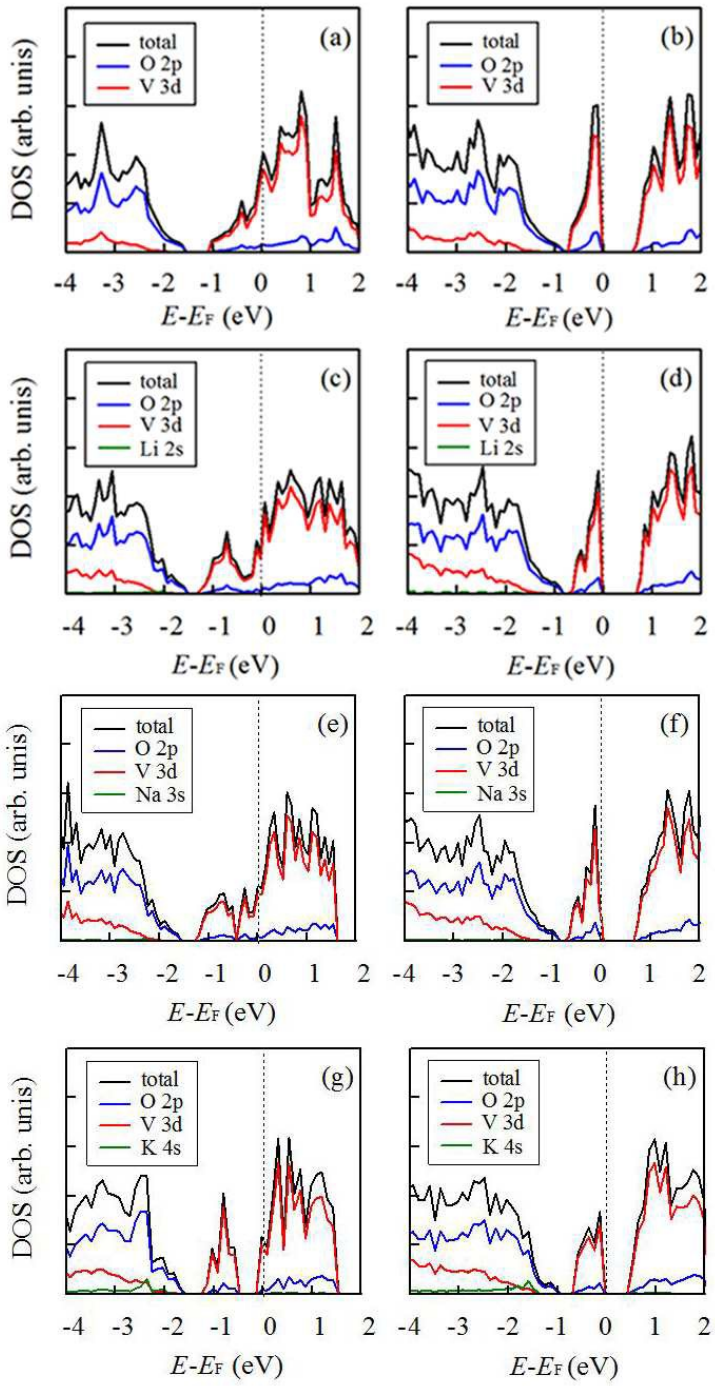

Fig. 3 The density of states (DOS) of pure VO_2(R) (a), pure VO_2(M) (b), Li-doped VO_2(R) (c), Li-doped VO_2(M) (d), Na-doped VO_2(R) (e), Na-doped VO_2(M) (f), K-doped VO_2(R) (g) and K-doped VO_2(M) (h). The zero point of the energy axis corresponds to the Fermi level E_F.

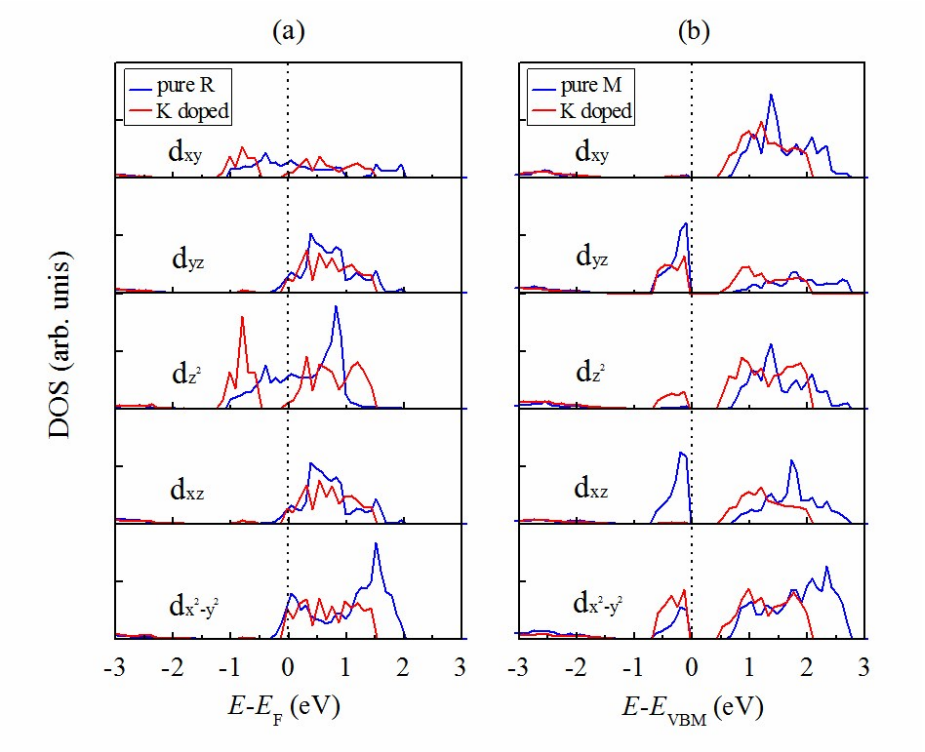

Fig. 4 The partial density of state (DOS) of the V-3*d* orbital of pure and K-doped VO_2(R) (a) and VO_2(M) (b). The zero point of the energy axis corresponds to the Fermi level E_F in (a) and valence band maximum E_{VBM} in (b), respectively.

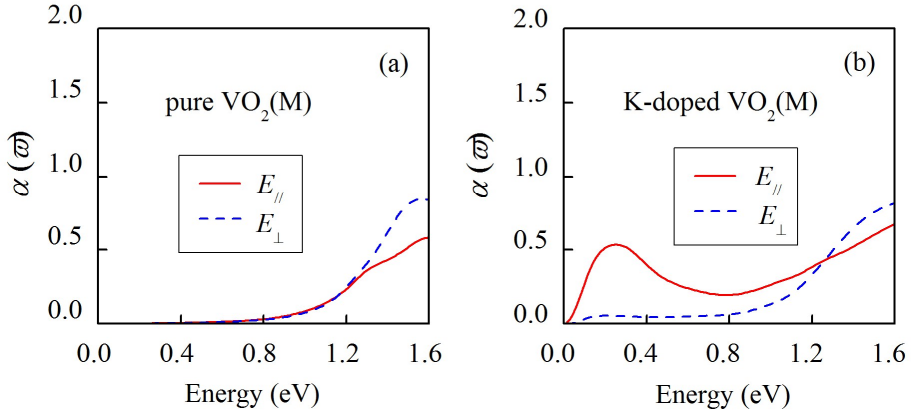

Fig. 5 The absorption spectra in the infrared spectral range obtained from first principles calculations for the pure VO_2(M) (a) and K-doped VO_2(M) (b). The absorption coefficient $\alpha(\omega)$ is given in 10^5 cm^{-1}.

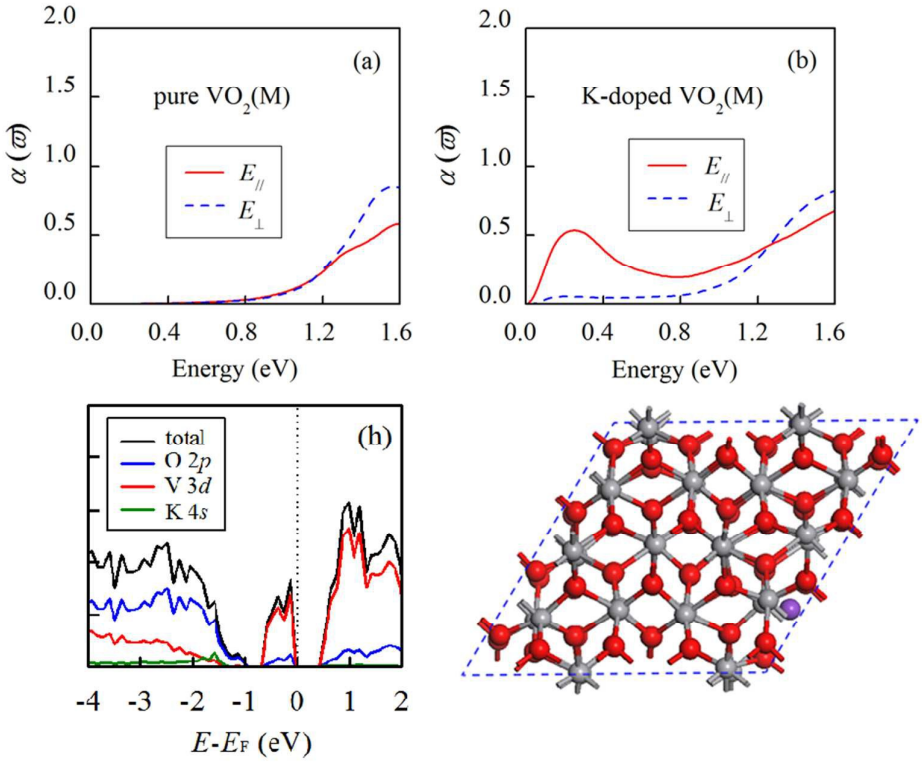

Our first-principles calculation indicates that K dopant with a doping level of 1 atomic percentage could reduce the phase transition temperature of VO_2 by 94 K. The calculated electronic structures and optical properties indicate that K can be selected as an appropriate doping element for VO_2, since it can effectively lower the phase transition temperature as well as enhance the near-infrared absorption.